Design and Characterization of CPW to Stripline Transition in LTCC for mm-wave Applications

A.Stefanescu[1], M.Lahti[2], A.C.Bunea[1], D.Neculoiu[1], T.Vaha-Heikkila[2]
[1] IMT-Bucharest, 32B, Erou Iancu Nicolae street, R-077190, Bucharest, Romania, alexandra.stefanescu@imt.ro
[2] VTT Technical Research Centre, Finland.

Abstract- **This paper presents the electromagnetic modeling and design of a vertical transition from coplanar waveguide to substrate embedded stripline for Low-Temperature Co-fired Ceramics (LTCC) technology. The commercial software package CST Microwave Studio was used. Several test structures with two vertical transitions connected by striplines of different lengths were designed, fabricated and measured. The comparison between simulated and measured data for the test structures shows a good agreement. The substrate embedded stripline effective permittivity is extracted from experimental results.**

I. INTRODUCTION

System-in/on-Package (SiP/SoP) technology is widely regarded as an excellent means of realizing very compact multifunctional modules. A variety of technologies can be employed, including Low-Temperature Co-fired Ceramic (LTCC), liquid crystal polymer, organic and thin film on glass, etc. As a result, the development of compact and low cost RF modules is possible for millimeter-wave (mm-wave) applications [1-3].

The three-dimensional (3-D) integration approach using multilayer LTCC technologies has emerged as an attractive solution due to its high level of compactness and mature multilayer fabrication capability. It enables integration of passive components including antennas, filters, couplers with MMICs in a single, cost-effective package. Passive structures, including transmission lines, can be placed on different layers and the processing of cavities and vias inside the substrate is possible. The 3-D modules can be innovatively designed and integrated at low cost.

LTCC technology offers stable and low-loss materials for mm-wave frequency domain and its advantages have already been demonstrated for mm-wave applications in the last few years, mainly up to the V-band (50 – 75 GHz) [4, 5]. Currently the highest frequency range where LTCC technology has been studied is 150 GHz [6].

To realize a successful RF/MW SiP/SoP module based on LTCC substrate technology accurate electromagnetic models based on mature process validation are a prerequisite.

Highly integrated microwave circuits require a combination of coplanar waveguide (CPW) and substrate embedded striplines (SL), thus requiring suitable wideband low-loss transitions between these two lines [7]. The transition from a CPW to SL line is asymmetrical and its S-parameters cannot be obtained directly by measurements using a probe station.

This paper serves several purposes. First, it presents the electromagnetic modeling and the design of a vertical transition from CPW to SL for V-band and W-band. According to the Radio Society of Great Britain, the W band covers the 75 – 110 GHz frequency range. Next, several test structures based on vertical transitions between the conductor-backed CPW and the embedded SL were designed and fabricated. Two transitions were connected "back-to-back" by SL transmission lines with three different lengths and measured up to 110 GHz. The substrate embedded SL effective permittivity is extracted from experimental results. Finally, a parametric study of the test structures is performed using electromagnetic simulations. The simulated results for different input values of the dielectric permittivity and loss tangent are compared.

II. DESIGN AND LTCC TECHNOLOGY

Miniaturization, low-loss interconnection and reduced process sensitivity have been considered as the most important issues for RF system integration. The miniaturization of different modules is pursued through vertical deployment of its elements using multilayer dielectrics. The major benefits of the LTCC technology are low conductor and dielectric losses, good thermal conductivity, stability, hermeticity, and cost efficiency. Disadvantages are related to the fabrication tolerances for the millimeter-wave domain.

In this work, the design is based on the VTT technology that uses the Ferro A6-M LTCC tape system with a fired tape thickness of 100 µm [4, 8]. The electrical parameters of the tape and conductor materials used in the design are: relative permittivity $\varepsilon_r = 5.9$ (+/- 0.2), loss tangent 0.001@20 Ghz, silver paste conductivity $\sigma = 3e7$ S/m, conductor thickness $t = 10$ µm. The main restrictions from the design rules are the minimum conductor widths and spacing of 100 µm. The diameter of all vias is 100 µm and the minimum spacing between two adjacent vias is 250 µm (centre to centre).

A 3-D view of the CPW-SL vertical transition is shown in Fig.1. A two step transition was chosen in the design. It has 3 dielectric tapes and 4 metallization layers: the backside ground layer, the stripline layer (used for the SL signal conductor), the slotted ground layer and the CPW layer.

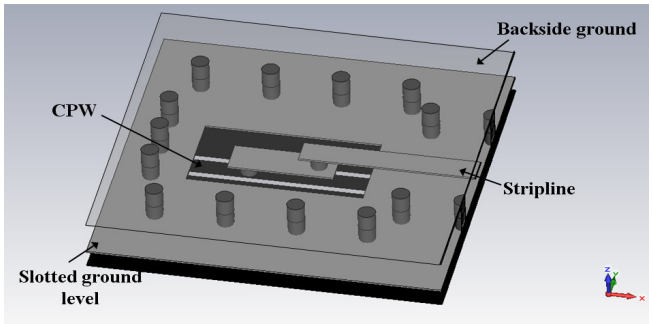

Figure 1. 3D view (backside) of the CPW-SL transition

At very high frequencies (up to 110 GHz) the modeling and design of the LTCC circuits is a challenge because the wavelength (1235 µm at 100 GHz, including the tape dielectric permittivity) have the same order of magnitude with the vertical transitions dimensions and the dimensions of other circuit components. The 0D (lumped elements) and even 1D (transmission lines) equivalent circuit modeling approach can no longer be used and full wave EM simulations must be employed in the design and optimization processes.

The vertical transition was modeled using the commercial software package CST Microwave Studio (MS) [9]. CST MS uses mainly time domain simulations. The port definition and S parameter extraction are optimized for electric field distribution (ideal for waveguide port and planar ports with multiple pins definition feature).

The combined effects of minimal line width and a high dielectric constant lead to values for the dielectric embedded transmission lines (microstrip, stripline) characteristic impedances that are lower than usual. For example, a characteristic impedance of 50 Ω is difficult to obtain for an embedded SL. Because the SL is used to feed other components, a width of 150 µm was used in the design (the characteristic impedance is about 28 Ω). Another 3-D view of the vertical transition is presented in Fig.2. The CPW port designed for "on wafer" measurement is visible. The CPW transmission line dimensions are 50 µm – 100 µm – 50 µm (gap – signal – gap) and the simulated corresponding impedance is about 52 Ω. The short ended CPW stub is intended to be used as DC return path in circuits with active components and as vertical transition tuning component.

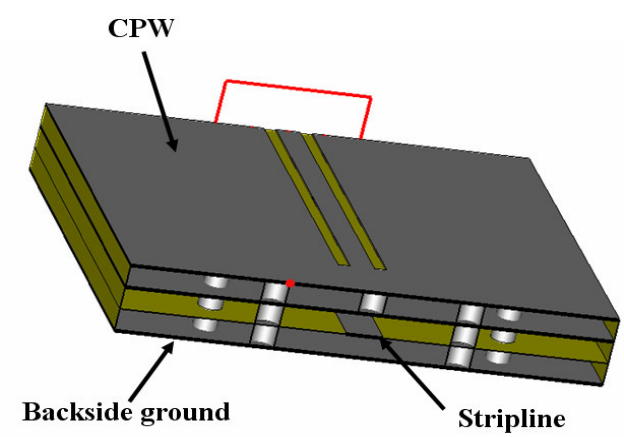

Figure 2. 3D view of the CPW-SL transition (input CPW-port view)

The signal conductors of the CPW and SL transmission lines are connected by vias in two steps. The vertical transition is surrounded by a screen of vias. These prevent the electromagnetic interference between adjacent components and connect ground planes placed on different tapes. The whole structure was optimized using the CST MS optimization engine. The main dimensions of the layout are shown in Fig. 3. The spacing between two adjacent vias in the lateral fences is 400 µm (centre to centre).

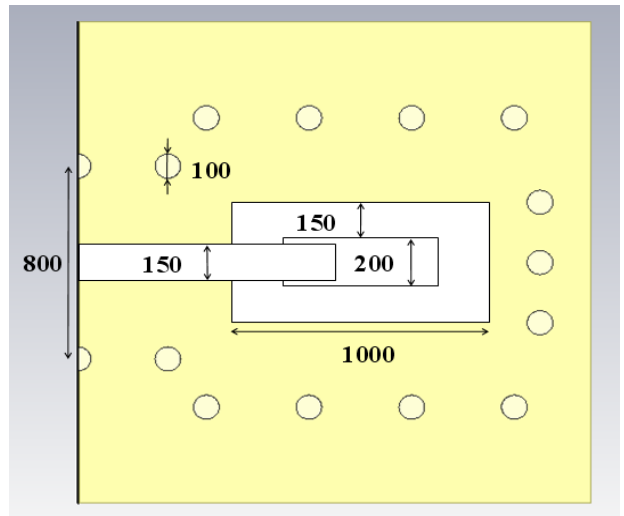

Figure 3. CPW-SL transition layout (stripline layer and slotted ground layer)

The simulated results for the optimized vertical transition are presented in Fig.4 and Fig.5. Fig.4 presents the transmission parameter (S_{21}) from 10 to 110 GHz. We can notice a resonance at about 67 GHz. Fig.5 presents the magnitude of the S parameters from 65 to 90 GHz, a frequency range interesting for applications such as automotive radars. The simulated performances of the vertical transition are very good in terms of low transmission losses and matching. We can observe a parasitic mode band pass filter. The resonance at 67 GHz is due to the resonant cavity created by the metallization layers and the vias fences. Fig.6 shows the electric field distribution in the plane situated halfway between the slotted ground layer and the stripline layer at 67 GHz.

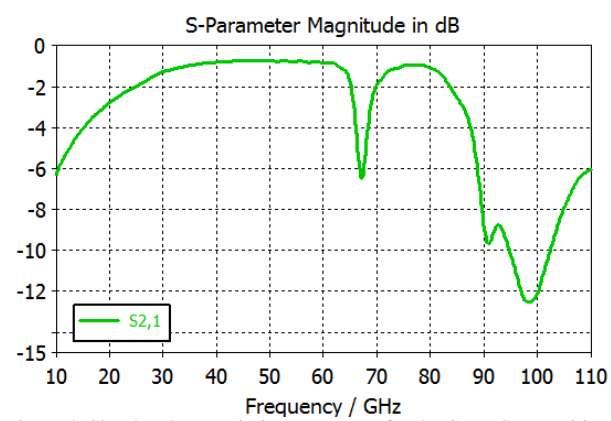

Figure 4. Simulated transmission parameter for the CPW-SL transition

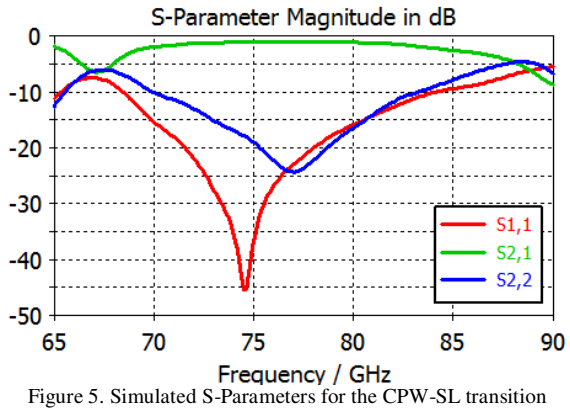

Figure 5. Simulated S-Parameters for the CPW-SL transition

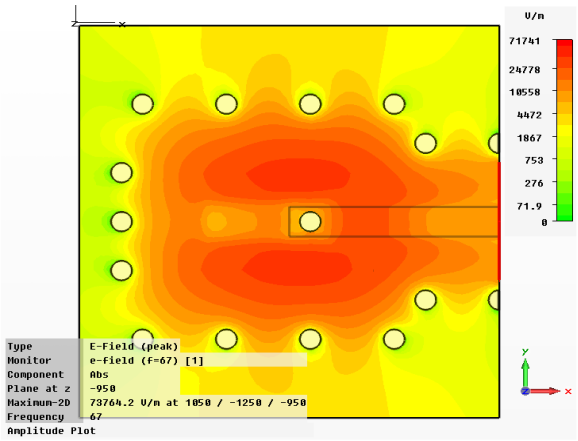

Figure 6. Electric field distribution at 67 GHz (see text)

III. Fabrication and Experiment

Three test structures were designed and fabricated: two vertical transitions placed back-to-back; two vertical transitions placed back-to-back separated by a SL 500 µm long (1 intermediate vias); two vertical transitions placed back-to-back separated by a SL 1000 µm long (3 intermediate vias). The photo of the fabricated structures is shown in Fig.7.

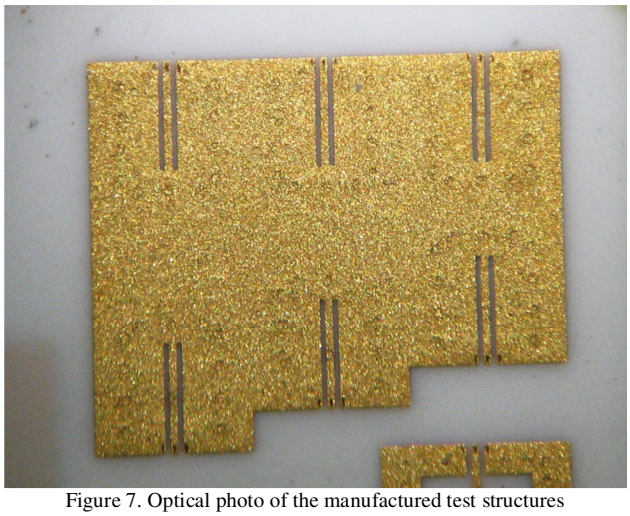
Figure 7. Optical photo of the manufactured test structures

The S-parameter measurements were carried out with a PM5 Suss Microtec "on wafer" probe station and Anritsu 37397D Vector Network Analyzer (VNA), equipped with 3742A-EW 65-110 GHz external modules. The standard SOLT calibration was used in the experiment. In the probe station, ground-signal-ground (GSG) probes with a 150 µm pitch were used, and measurements were conducted up to 110 GHz.

Fig. 8 shows the comparison between the simulated and experimental results for the two vertical transitions placed back-to-back, the vertical transitions separated by a SL 500 µm long and the vertical transitions separated by a SL 1000 µm long, respectively. The agreement between simulations and experiments is very good.

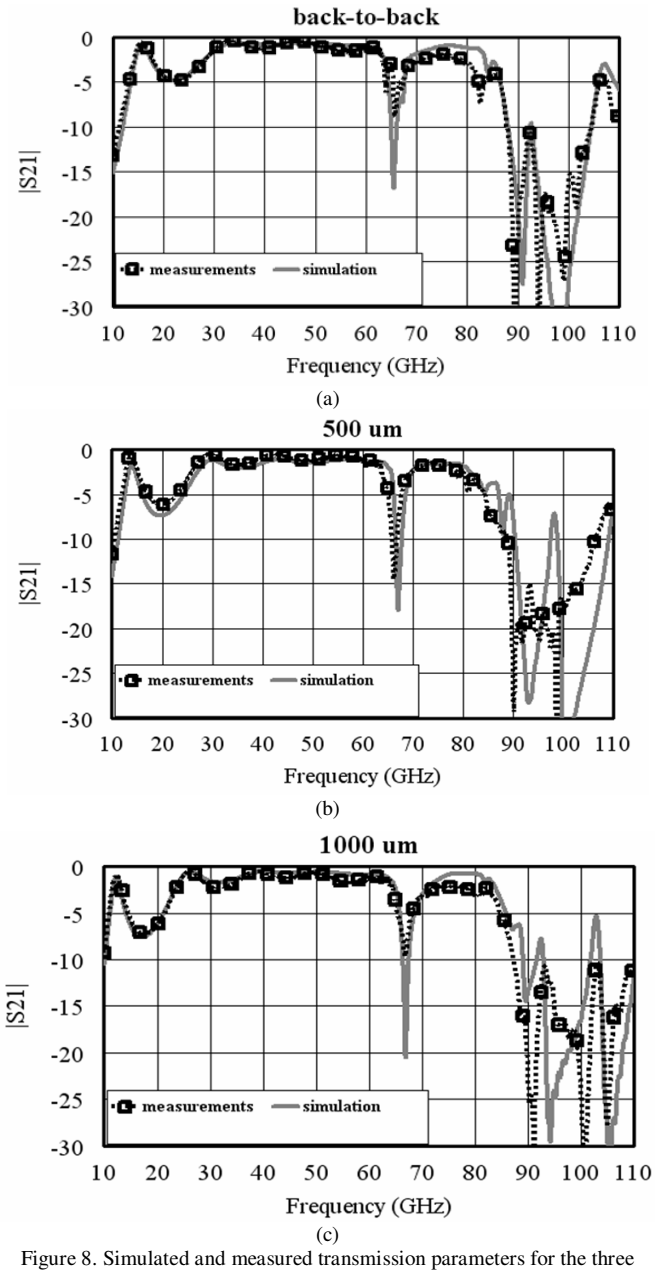

Figure 8. Simulated and measured transmission parameters for the three CPW-SL-CPW test structures

From the simulations and the experimental results, the effective permittivity of the embedded SL is extracted using the method presented in [10]. Considering the S parameters for two test structures with different length for the stripline L_A and L_B, the propagation constant of the SL can be calculated with (1).

$$\gamma = \frac{1}{\Delta L} \arg ch \left(\frac{S_{11}^B S_{22}^A + S_{11}^A S_{22}^B - \Delta_A - \Delta_B}{2 - S_{21}^B S_{12}^A} \right) \quad (1)$$

where

$$\Delta L = L_B - L_A$$
$$\Delta A = S_{11}^A S_{22}^A - S_{12}^A S_{21}^A$$
$$\Delta B = S_{11}^B S_{22}^B - S_{12}^B S_{21}^B$$

The propagation constant is a complex number given by (2), where α is the attenuation constant and β is the phase constant.

$$\gamma = \alpha + j\beta \quad (2)$$

The effective permittivity of SL transmission line section can be computed using (3).

$$\varepsilon_{eff} = \frac{\mathrm{Im}(\gamma)}{\omega^2 \mu_0 \varepsilon_0} \quad (3)$$

where ω is the angular frequency, ε_0 and μ_0 are the vacuum permittivity and permeability, respectively.

Fig. 9 shows the comparison between the variation of the effective permittivity extracted from the simulated and experimental results versus frequency. The agreement is good and close to the value of the relative permittivity of 5.9 used in the simulations. It can be noticed that there is a large deviation from this value at the frequencies corresponding to the parasitic resonances and high transmission losses (see Fig. 8).

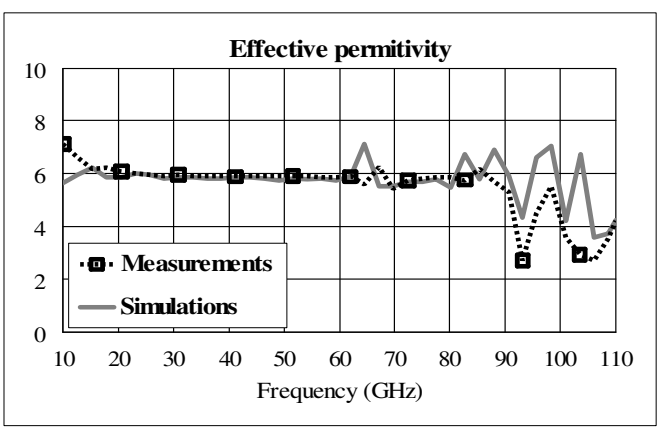

Figure 9. Effective permittivity vs. frequency extracted from the simulated results (continuous gray line) and measurement results (dotted black line, square markers)

IV. Parametric Study

The comparison between simulated and experimental data was presented in the previous section and the agreement was very good up to 60 GHz. For the 65-90 GHz frequency range there is a slight increase in losses (about 0.5 … 1.5 dB at 77 GHz). In order to identify the cause of these losses we performed a parametric study using electromagnetic simulation with CST MS. The tape relative permittivity was varied between 5.7 and 6 and the results are presented in Fig. 10 (whole frequency range) and Fig. 11 (65 – 90 GHz). A slight decrease of the resonance frequency of the parasitic modes can be observed with the increase of the relative permittivity.

The effect of the tape losses was also investigated and the loss tangent was varied between 0.001 …. 0.003. Almost no effect was observed on the simulated transmission parameter.

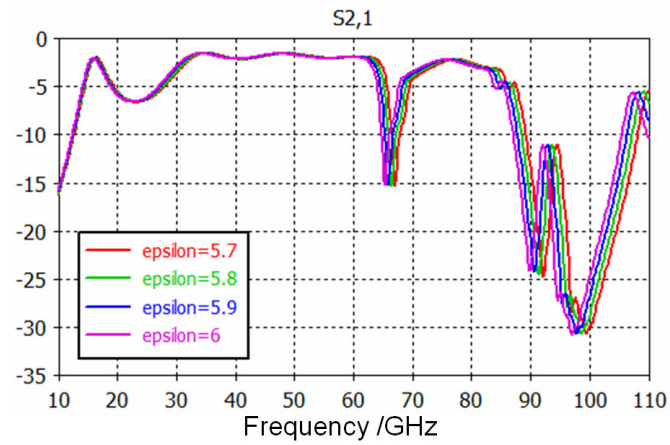

Figure 10. Parametric study of the transmission parameters for the CPW-SL-CPW structure

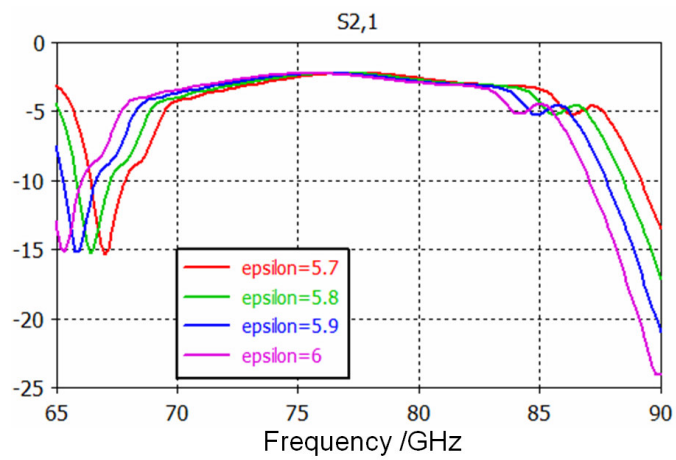

Figure 11. Parametric study of the transmission parameters for the CPW-SL-CPW structure – detail for the 65-90 GHz frequency range

V. Conclusions

The electromagnetic modeling and design of a vertical two-step CPW to stripline transition for frequencies up to 110 GHz were described. The transition was optimized for minimum transmission losses and good matching using the electromagnetic simulation software CST Microwave Studio.

Three structures consisting of back-to-back connected transitions with different stripline lengths were investigated and then manufactured in LTCC technology.

The CPW-SL-CPW structures were measured with a PM5 Suss Microtec "on wafer" probe station and Anritsu 37397D Vector Network Analyzer (VNA), equipped with 3742A-EW 65-110 GHz external modules. The simulated and measured results are in good agreement.

The effective permittivity of the embedded stripline was extracted for both simulation and measured data showing good agreement with the value used in simulations (5.9) up to 60 GHz.

In order to identify the causes for the discrepancies in transmission losses at higher frequencies, a parametric study was performed for the tape parameters, relative permittivity and loss tangent.

ACKNOWLEDGMENT

The authors would like to acknowledge the European Union for the funding and continuous support of the ICT-project MEMS-4-MMIC, grant agreement number 224101, 7th Framework Program. The Romanian authors acknowledge the support of the Romanian Ministry of Education, Research, Youth and Sports (project 18/2009 "MEMS 4 MMIC").

REFERENCES

[1] D.Liu, B.Gaucher, U.Pfeiffer and J.Grzyb, "Advanced millimeter-wave technologies : antennas, packaging and circuits", John Wiley & Sons, 2009.

[2] K.Kuang et al. (eds), "RF and Microwave Microelectronics Packaging", chap.9, Springer Science, 2010

[3] J.-H. Lee, G. DeJean, S. Sarkar, S. Pinel, K. Lim, J. Papapolymerou, J. Laskar, and M. M. Tentzeris, "Highly integrated millimeter-wave passive components using 3-D LTCC system-on-package (SOP) technology", *IEEE Trans. Microw. Theory Tech.,* vol. 53, no. 6, pp. 2220–2229, Jun. 2005.

[4] A.Lamminen, J.Säily, and A.R.Vimpari, "60-GHz Patch Antennas and Arrays on LTCC with Embedded-Cavity Substrates", *Antennas and Propagation.,* vol. 56, no. 9, pp. 2865–2874, Sept. 2008.

[5] J.-H.Lee, N.Kidera, G.DeJean, , S. Pinel, J. Laskar, and M. M. Tentzeris, "A V -Band Front-End With 3-D Integrated Cavity Filters/Duplexers and Antenna in LTCC Technologies", *IEEE Trans. Microw. Theory Tech.,* vol. 54, no. 7, pp. 2925–2936, July. 2006.

[6] A. Khalil, D. Passerieux, D. Baillargeat, S. Verdeyme, L. Rigaudeau, and J. Puech, "150 GHz bandpass filter using LTCC technology," *IEEE Microw. Wireless Compon. Lett.*, vol. 19, no. 7, pp. 455–457, Jul. 2009.

[7] S.Bulja, D. Mirshekar-Syahkal, "Novel Wideband Transition Between Coplanar Waveguide and Microstrip Line", *IEEE Trans. Microwave Theory Tech.*, vol. 58, no.7, pp. 1851-1857, July 2010.

[8] D.Neculoiu, AA.Muller, A.Stefanescu, T.Vaha-Heikkila, I.Petrini, C.Buiculescu, "Electromagnetic Design of W-Band Circuits in LTCC Technology", *Proceeding of CAS*, Sinaia, Romania, p.287, 2010.

[9] www.cst.com

[10] B.Bianco, M.Parodi, "Determination of the propagation constant of uniform microstrip lines", Alta Frequenza, vol.XLV, No.2, Feb1976, pp.107 - 110.